Nonadiabatic unimolecular reactions. III. Dissociation mechanisms of methylnitrite and deuterated methylnitrite ions

B. Leyh-Nihant and J. C. Lorquet

Citation: The Journal of Chemical Physics **88**, 5606 (1988); doi: 10.1063/1.454571
View online: http://dx.doi.org/10.1063/1.454571
View Table of Contents: http://scitation.aip.org/content/aip/journal/jcp/88/9?ver=pdfcov
Published by the AIP Publishing

Articles you may be interested in

Quantum dynamics of unimolecular dissociation reaction HFCO→HF+CO
J. Chem. Phys. **109**, 9783 (1998); 10.1063/1.477648

The unimolecular decomposition rates of energy selected methylnitrite and deuterated methylnitrite ions
J. Chem. Phys. **78**, 3767 (1983); 10.1063/1.445152

Unimolecular reaction paths of electronically excited species. III. Production of CH+ 3 ions from CH3OH+ as an example of isolated state dissociation
J. Chem. Phys. **77**, 4522 (1982); 10.1063/1.444401

Applications of the Quantum Mechanical Green's Function Technique to Unimolecular Dissociation Reactions. V
J. Chem. Phys. **54**, 416 (1971); 10.1063/1.1674624

The Mechanism of Unimolecular Reactions
J. Chem. Phys. **21**, 1093 (1953); 10.1063/1.1699115

This article is copyrighted as indicated in the article. Reuse of AIP content is subject to the terms at: http://scitation.aip.org/termsconditions. Downloaded to IP: 139.165.205.242 On: Fri, 04 Sep 2015 14:32:57

Nonadiabatic unimolecular reactions. III. Dissociation mechanisms of methylnitrite and deuterated methylnitrite ions

B. Leyh-Nihant[a] and J. C. Lorquet[b]
Département de Chimie, Université de Liège, Sart-Tilman, B-400 Liège 1, Belgium

(Received 13 November 1987; accepted 21 January 1988)

At low energies, methylnitrite ions dissociate via two channels giving rise to $CH_3O + NO^+$ or to $[CH_3O^+] + NO$ fragments. Peculiar characteristics have been detected in the dissociation of energy-selected parent ions, viz., remarkably low rate constants, one of which is found to remain insensitive to an increase of the internal energy, and large isotope effect. These peculiarities are accounted for by a statistical, nonadiabatic model. *Ab initio* calculations, confirmed by multipolar expansions reveal that the potential energy curves which correlate to these two dissociation asymptotes cross. The crossing takes place at a large value along the reaction coordinate R, indicating a long-range interaction. Production of the $CH_3O + NO^+$ fragments results from a simple bond cleavage taking place on a single diabatic surface. On the other hand, production of $[CH_3O^+] + NO$ fragments is brought about by a transition from one diabatic surface to the other. It leads to deformed methoxy ions which immediately rearrange to the much more stable H_2COH^+ structure. The nonadiabatic rate constant has been calculated by a statistical method. The contribution of each channel is weighted by a transmission coefficient which is equal to the nonadiabatic transition probability. Implementation of this statistical treatment requires partitioning the set of degrees of freedom as follows: $\{R, y, \mathbf{d}, \mathbf{v}\}$. It is necessary to withdraw the isomerization mode y from the statistical treatment, because the equilibrium positions along this coordinate are very different in each electronic state. Physically, this means that the reaction involves tunneling from one surface to the other along the displaced degree of freedom y. The large isotope effect has a double origin: part of it (a factor of ~ 9) results from tunneling along y; the remainder (an additional factor of 3) comes from the usual RRKM-like effect on the densities of states. The degrees $\mathbf{d}$ constitute a set of four low-energy bending modes which form a sink for the internal energy. The nonadiabatic transition probability is determined by the off-diagonal matrix element $V_{12}(R_c)$. Effective potential energy curves have been calculated by extending the Quack and Troe method to nonadiabatic reactions. It turns out that the excitation of the set $\mathbf{d}$ leads to a decrease of $V_{12}(R_c)$ and hence to a decrease of the nonadiabatic transmission coefficient. This accounts for the weak dependence of the rate constants $k_{CH_3O^+}$ and $k_{CD_3O^+}$ vs the energy (at least above a certain energy threshold).

I. INTRODUCTION

The unimolecular dissociation of the methylnitrite ion has aroused great interest among several groups.[1-8] Surprising effects have been observed, and the point at issue is whether they indicate a breakdown of the basic assumptions of the statistical theory of unimolecular reactions[9] (RRKM theory—also termed QET by many mass spectrometrists). Does the system reach a state of microcanonical equilibrium before reacting? Does one have to deal with some unconventional transition state? Is the reaction nonadiabatic, i.e., does it involve participation of several electronic states?

The basic experimental information is a PEPICO study carried out by Meisels *et al.*[1] This method[1,2,4,10] allows a determination of the breakdown diagram (giving the yield of fragmentation), sometimes also of the dissociation rate constants, as a function of the internal energy of the molecular ion. At low internal energies, two channels are open,

$$CH_3ONO^+ \rightarrow [CH_3O]^+ + NO \quad (AE = 10.69\ \text{eV}), \tag{1.1}$$

$$CH_3ONO^+ \rightarrow CH_3O + NO^+ \quad (AE = 10.83\ \text{eV}). \tag{1.2}$$

[For the time being, we do not wish to discuss the exact structure of the charged fragment produced in reaction (1.1) and we use brackets to indicate that we consider its global formula only]. The energetic data have been slightly revised by Baer and Hass.[4]

The remarkable features exhibited by this pair of reactions, which have been recently reinvestigated by Baer and Dutuit,[8] can be summarized as follows:

(a) Although both reactions have similar thermodynamic thresholds, there is an unexpected degree of specificity in favor of reaction (1.2), i.e., in favor of the most endoergic reaction. This is very surprising if both channels have the same reaction coordinate. Reaction (1.2) is thought to take place via simple bond cleavage without any reverse energy

[a] Aspirant F.N.R.S., Belgium.
[b] To whom correspondence should be addressed.

 0021-9606/88/095606-14$02.10 © 1988 American Institute of Physics

This article is copyrighted as indicated in the article. Reuse of AIP content is subject to the terms at: http://scitation.aip.org/termsconditions. Downloaded to IP: 139.165.205.242 On: Fri, 04 Sep 2015 14:32:57

barrier,[2] but the situation is much less clear for the other channel.

(b) Collision induced dissociation of the charged species produced in reaction (1.1) reveals[3,4] that these ions have the structure H_2COH^+. Hence, in contradistinction to reaction (1.2), the low-energy channel is not a simple bond cleavage but involves some rearrangement. However, Burgers and Holmes point out[3] that the transient production of methoxy CH_3O^+ ions cannot be ruled out. This turns out to be an essential point in the mechanism which will be studied in detail below.

(c) A comparison between the breakdown diagrams of CH_3ONO^+ and CD_3ONO^+ reveals a surprisingly strong isotope effect. The relative abundance of $[CH_3O]^+$ reaches a maximum value of 60% at 10.85 eV and decreases rapidly to a value of zero. In sharp contrast, the $[CD_3O]^+$ ions are produced with a maximum yield which, according to Gilman *et al.*'s measurements, is of 5% only at 11 eV.

(d) Reaction (1.1) take place with a rate constant of about $10^6\ s^{-1}$. Since the dissociation energy is of the order of 0.5 eV only[4] or even less,[1] such a small rate cannot be accounted for by RRKM theory, at least in its usual version.

(e) Even more surprising is the comparison between the rate constants $k_{CH_3O^+}$ and $k_{CD_3O^+}$ of channel (1.1). The latter is found to remain constant over a large range of internal energies. (However, this range is certainly less extended than that indicated in Ref. 1: distortion by an apparatus function certainly takes place).[11] Again, such a behavior is at odds with RRKM theory which predicts a regular increase of the rate constant with the internal energy. Moreover, the data of Ref. 1 suggest an isotope effect which increases with the internal energy.

(f) Reactions (1.1) and (1.2) are characterized by different rate constants, as shown by the shape of their time-of-flight peaks.[1,8] The former falls into the microsecond time scale, whereas production of NO^+ ions takes place with a much smaller lifetime (10^{-7} s or less). According to the laws of macroscopic kinetics, this is evidence that the two fragmentations do not take place from a common intermediate.

Meisels *et al.*[1] conclude that reactions (1.1) and (1.2) cannot be described by the RRKM/QET theory and involve probably a surface crossing. However, Ogden *et al.*[2] conclude from kinetic energy release measurements that production of NO^+ ions can be accounted for by a statistical theory. Ferguson[7] has made a crude estimate of the isotope effect and proposes an alternative explanation for effect (c). He suggests that the ions of mass 34 formed in the dissociation of the perdeuterated isotope be D_2NO^+ rather than D_3CO^+ or D_2COD^+.

In a detailed analysis, Baer and Hass[4] postulate straight away that the ions react in a state of microcanonical equilibrium. They start from observation (f) and suggest that the CH_3ONO^+ ions should exist in at least two isomeric structures, each of which giving rise to a specific reaction channel. Their mechanism involves a competition between a direct fragmentation represented by Eq. (1.2) and isomerization toward some more stable structure dissociating into H_2COH^+. They carried out *ab initio* calculations which reveal indeed that a particular structure $HNC(OH)_2^+$ is characterized by a surprising stability [see also Ref. 5(b)]. However, the height of the barrier along the isomerization path could not be estimated and had to be treated as an adjustable parameter in the RRKM calculations. Such a mechanism, which involves four rate constants instead of 2, has been shown in earlier studies[4,10] to account for the behavior of several other ions. This is certainly an interesting suggestion, but it is doubtful that this mechanism can also account for the isotope effect and for the constancy of $k_{CD_3O^+}$.

Very recently, Baer and Dutuit[8] have remeasured the breakdown graphs with a better energy resolution using dispersed synchrotron radiation as a light source. Their results are sometimes very different from those obtained by Meisels *et al.* (The discrepancies will be discussed later on in Sec. X.)

In conclusion, in front of such a complex problem, it is interesting to see whether another model could not turn out to be more appropriate.

II. THE NONADIABATIC MODEL

The fact that the products of reactions (1.1) and (1.2) differ by the location of the positive charge suggests an analogy with the celebrated alkali halide problem[12] in which the dissociation process is controlled by a curve crossing between a covalent and an ionic structure. As a matter of fact, the products of reactions (1.1) and (1.2) *must* correlate to two different electronic states of the methylnitrite ion. However, for the reaction to proceed through a nonadiabatic interaction, the diabatic potential energy curves must cross in a region which is visited by the reactive trajectories. Let R_C be the distance at which this crossing takes place, measured along a coordinate R which is the separation between the centers of the two fragments. The larger R_C, the weaker the interaction between the diabatic curves. Conversely, the smaller R_C, the more appropriate the adiabatic representation.

A precious first indication can be obtained as follows. Consider the situation where the fragments are separated by an infinite distance. The CH_3O radical is known to exist in two stable structures[13]: H_3CO and H_2COH. The potential energy curve along the isomerisation reaction path (which involves migration of a hydrogen atom from carbon to oxygen) has been determined by reliable *ab initio* calculations.[13,14] On the other hand, the CH_3O^+ ion can exist in the methoxy H_3CO^+ geometry in the triplet state only. The lowest singlet state is unstable for this geometry and collapses into the very stable hydroxymethylene H_2COH^+ structure without an activation energy barrier.[3,15–18]

The set of diabatic potential energy curves when the pairs of fragments are separated by an infinite distance is represented in Fig. 1. There is indeed a crossing between them. As the partners draw nearer, the diabatic potential energy surfaces are shifted and deformed, but the crossing between the first two electronic states of CH_3ONO^+ subsists.

A complementary piece of information comes from a study of the long range forces between the fragments (Fig. 2). Starting from the lower dissociation asymptote (1.1), the positive charge on the $[CH_3O]^+$ ion interacts with the small

This article is copyrighted as indicated in the article. Reuse of AIP content is subject to the terms at: http://scitation.aip.org/termsconditions. Downloaded to IP: 139.165.205.242 On: Fri, 04 Sep 2015 14:32:57

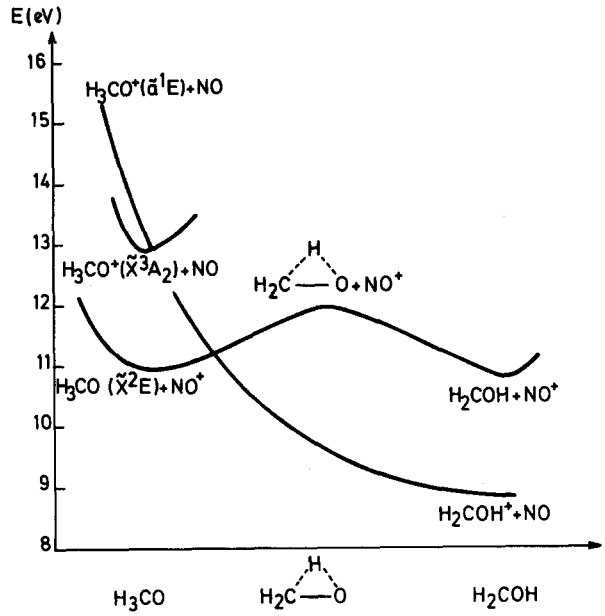

FIG. 1. Diabatic potential curves along the isomerization coordinate when the pairs of fragments are separated by an infinite value of coordinate R.

dipole moment of the NO radical: the corresponding potential energy curve can be expected not to depend strongly on the coordinate R used in the multipolar expansion. On the other hand, for the upper dissociation asymptote (1.2), the positive charge carried by the NO^+ ion interacts strongly with the large dipole moment (2.1 D [19]) of the CH_3O radical. This gives rise to a stabilizing charge–dipole interaction which varies as $-R^{-2}$. Now, just as in the alkali halide problem,[12] the energy difference ΔE_∞ between the asymptotes (1.1) and (1.2) is very small (0.14 eV according to Gilman *et al.*,[1] 0.09 eV according to Baer and Hass[4]). An intersection is thus expected for a rather large value of the reaction coordinate R (Fig. 2).

Therefore, we propose a model based on a weak interaction between two diabatic potential energy surfaces. The

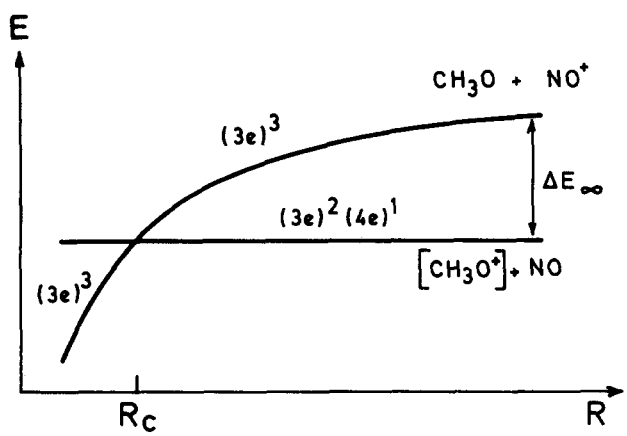

FIG. 2. Schematic potential curves along the distance R between the centers of mass of the fragments. The value of ΔE_∞ is equal to 0.14 eV according to Ref. 1 and to 0.09 eV according to Ref. 4.

fragments $CH_3O + NO^+$ corresponding to the higher asymptote (1.2), result from a simple bond cleavage taking place on a single *diabatic* energy surface. On the other hand, production of $[CH_3O]^+ + NO$ fragments [the lower asymptote (1.1)] is induced by a transition from one diabatic surface to the other. From the position of the crossing along the isomerisation coordinate (Fig. 1), one expects the $[CH_3O]^+$ ions to be born with a deformed geometry, intermediate between a C_{3v} methoxy and a bridged structure, and to rearrange immediately to the more stable hydroxymethylene isomer H_2COH^+, as suggested by Burgers and Holmes.[3] In order to put this mechanism on a firmer basis, a few *ab initio* calculations have been carried out.

III. *AB INITIO* CALCULATIONS

All our calculations have been done with the MOLALCH system of programs[20] in the point group C_s. The AO basis set for the carbon, oxygen, and nitrogen atoms was the standard Huzinaga–Dunning[21] (9*s*5*p*/3*s*2*p*) set of Cartesian Gaussians. For the hydrogens, the (4*s*/2*s*) set was used with a scaling factor of 1.2. Since the interaction to be studied takes place at large values of the reaction coordinate, it is appropriate to adopt as a one-electron basis set the SCF molecular orbitals (MOs) of the fragments. The Slater determinants constructed on these MOs are then introduced into a configuration interaction (CI) calculation. In order to get symmetry-consistent results, we have carried out our SCF calculations on fictitious electronic configurations with noninteger occupation numbers, i.e., $(7a')^{0.5}\ (2a'')^{0.5}$ for the NO fragment and $(7a')^{1.5}\ (2a'')^{1.5}$ for the CH_3O radical. Two basis sets of MOs were used (corresponding either to the fragments CH_3O and NO^+, or to the fragments $[CH_3O]^+$ and NO). The latter choice can be expected to generate better results than the former, because the MOs ($14a'$) and ($4a''$) (which are occupied in CH_3ONO^+) result from the occupied ($7a'$) and ($2a''$) MOs of the NO fragment.

In the C_{3v} point group, the leading electronic configuration of CH_3ONO^+ along the higher asymptote (1.2) is $(3e)^3$; it correlates diabatically with the ground state $\tilde{X}\,^2E$ (Fig. 2). Along the lower asymptote (1.1), the leading term in the CI expansion is $(3e)^2\ (4e)^1$. It correlates diabatically with the first ^2E excited state of CH_3ONO^+. The surface crossing which has been discussed in Sec. II results from this correlation. It persists in the C_s point group within both the $^2A'$ and $^2A''$ representations when the molecule is deformed.

For setting up the $^2A'$ CI matrices, four reference configurations were defined: $(13a')^1\ (3a'')^2$; $(13a')^1\ (3a'')^1\ (4a'')^1$; $(13a')^2\ (14a')^1$; and $(14a')^1\ (3a'')^2$. All the single excitations generated from these four reference configurations (excluding the four core orbitals and the top four virtual MOs) were included to generate a first $^2A'$ matrix built on 1609 configuration state functions (CSFs). A second $^2A'$ matrix was generated which, in addition, included all the doubly excited configurations generated in the ($13a'$, $3a''$, $14a'$, and $4a''$) shell. This gave rise to a set of 2510 CSFs. The corresponding $^2A''$ matrices were generated in a similar way.

These are relatively crude calculations which, for very large values of the reaction coordinate R (say from 26 to 5

This article is copyrighted as indicated in the article. Reuse of AIP content is subject to the terms at: http://scitation.aip.org/termsconditions. Downloaded to IP: 139.165.205.242 On: Fri, 04 Sep 2015 14:32:57

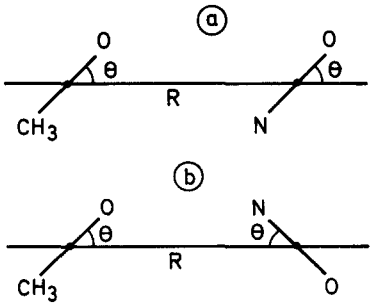

FIG. 3. Bending motions for large values of R: the angle θ is measured respective to the line connecting the centers of mass of the fragments.

Å), should generate potential energy curves of SCF (or slightly better than SCF) quality. Since the wave functions are generated by a common CI calculation, it will be possible (in Sec. V) to estimate the off-diagonal matrix element required for the calculation of the transition probabilities. No attempt was made to estimate the energy gap ΔE_∞ between the two asymptotes (1.1) and (1.2). This would require a much larger basis set of AOs and a better calculation of correlation energies.

A. *R* dependence

Several cross sections along the distance R between the centers of mass of the two fragments (henceforth referred to as the reaction coordinate) were calculated with R ranging between 5 and 26 Å. This was done, first, for a C_{3v} geometry of the CH_3ONO^+ supermolecule. Secondly, for a C_s geometry in which one of the HCO angle was given a value of 85°, roughly corresponding to the deformed geometry at which the $[CH_3O]^+$ ion is supposed to be generated (see Fig. 1). Several sets of CI calculations were carried out. As expected, the asymptotic energy gap ΔE_∞ was found to depend very sensitively on the possible options in the calculation (size of the CI matrix, nature of the MOs and internal geometry of the CH_3O or CH_3O^+ fragment). However, the potential energy curves generated by the various combinations remained remarkably parallel in the range of internuclear distances indicated.

Although our calculations are totally inadequate to determine ΔE_∞, they give us nevertheless a good approximation of the shape of the diabatic potential energy curves. If the latter are translated so that ΔE_∞ is equal to 0.14 eV, the two curves are found to cross at a value $R_c \simeq 8$ Å, i.e., a value at which our calculations can be expected to be reliable. Furthermore, as explained in Sec. IV, the results are consistent with a multipolar expansion.

B. Angular dependence

A second series of cross sections was calculated as a function of θ, the angle between a line joining the centers of mass of the two fragments and the principal axis of these fragments (Fig. 3). This bending motion, which later on will be found to play a leading role in the dynamics (Sec. VII), splits the degeneracy of the ^2E states and transforms them into a pair of $^2A'$ and $^2A''$ states. As shown in Fig. 4, the effect on the $(3e)^3$ state is much more pronounced than that on the $(3e)^2\,(4e)^1$ state. Here again, these *ab initio* results can be accounted for by a multipolar expansion, as shown in the next section.

IV. MULTIPOLAR EXPANSIONS

At the large internuclear distances which have been considered so far, exchange contributions can be neglected and the interaction energy can be expressed as a multipolar expansion. The purpose of the present section is to check the

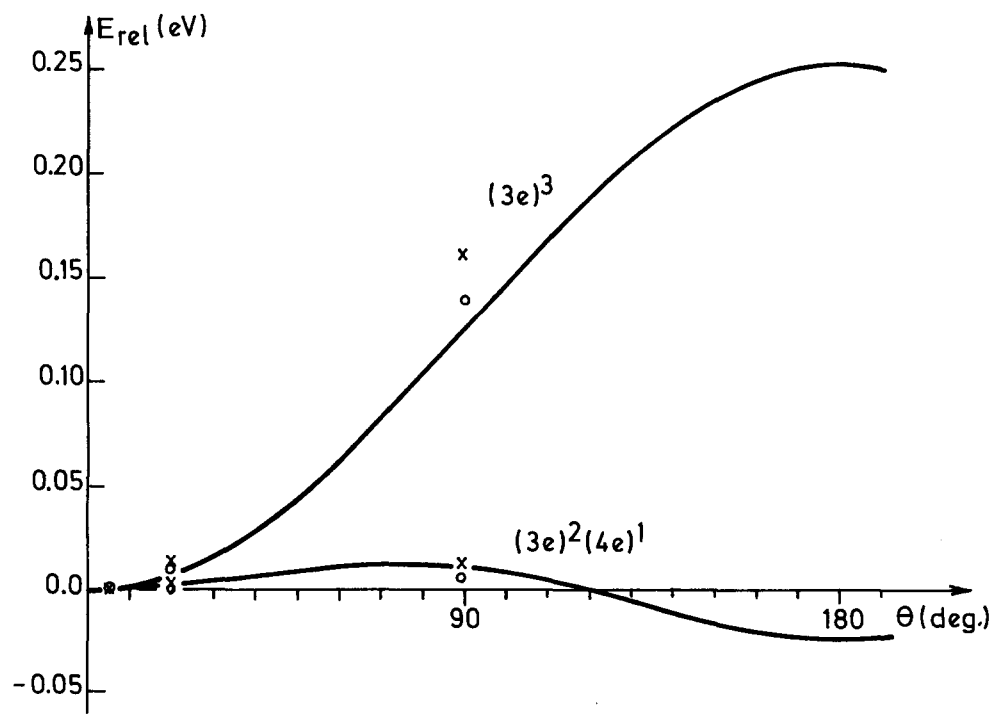

FIG. 4. Potential energy curves along the bending coordinate θ calculated for $R = 8$ Å. The crosses and open circles represents the results of *ab initio* calculations for the A′ and A″ states, respectively. The full curves result from the multipolar expansions [Eqs. (4.2) and (4.4), respectively].

This article is copyrighted as indicated in the article. Reuse of AIP content is subject to the terms at: http://scitation.aip.org/termsconditions. Downloaded to IP: 139.165.205.242 On: Fri, 04 Sep 2015 14:32:57

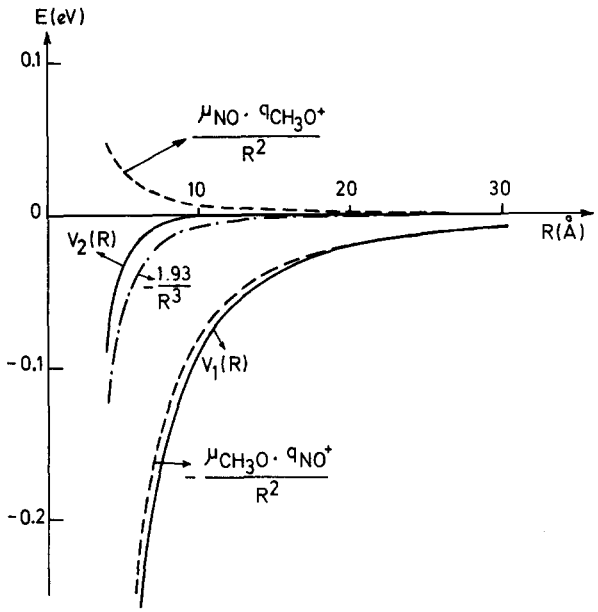

FIG. 5. Multipole expansions of the *ab initio* potentials $V_1(R)$ and $V_2(R)$ [Eqs. (4.1) and (4.3)] for the two states $(3e)^3$ and $(3e)^2\,(4e)^1$, respectively. The predominant contributions are represented in broken lines.

internal coherence between these expansions and *ab initio* cross sections calculated along R and θ.

A. The $(3e)^3$ configuration

The potential energy curve calculated *ab initio* as a function of R (Fig. 5) can be fitted by the expansion

$$V_1(R) = -1.0642R^{-2} - 2.1993R^{-3} - 0.1472R^{-4}, \tag{4.1}$$

where V and R are expressed in atomic units. Figure 5 shows that the contribution of the $-R^{-2}$ term (which describes the charge–dipole interaction) is by far dominant.

The complete expression for a charge–dipole interaction including angular dependence is

$$V(R,\theta) = \mu q R^{-2} \cos\theta. \tag{4.2}$$

Figure 4 shows that for a value of $R = 8$ Å, there is good agreement between Eq. (4.2) and the *ab initio* results. A value of 2.7 D for the dipole moment of CH_3O can be deduced from this comparison, in satisfactory agreement with the value $2.12D$ calculated by Jackels.[19]

B. The $(3e)^2\,(4e)^1$ state

Our *ab initio* calculations can be fitted in a similar way to the expansion (with V and R in a.u.)

$$V_2(R) = 0.0973R^{-2} - 1.9314R^{-3} - 0.0705R^{-4}. \tag{4.3}$$

Figure 5 shows that the first two terms dominate and, moreover, cancel each other so that the resulting potential curve is remarkably flat over a large range of internuclear distances. The positive term in R^{-2} accounts for an interaction between the positive charge carried by the CH_3O^+ point charge and the weak dipole moment of $0.25D$ (polarized N^+O^-). This compares well with previous SCF calculations which predict a dipole moment of $0.27D$ (N^+O^- polarity).[22] As frequently observed, the introduction of CI (including doubly excited configurations) reverses the sign of the dipole moment and predicts values of $0.12D$ and $0.14D$[22,23] with N^-O^+ polarity. This comparison agrees with our view that the present calculations generate potential energy curves at the SCF level only.

TABLE I. Absolute values of the coupling matrix element for different positions of the crossing point.

R_C (Å)	$\lvert V_{12}\rvert$(a.u.)
5.33	5.3×10^{-4}
7.33	2.1×10^{-6}
9.33	2.3×10^{-11}
11.33	1.7×10^{-17}

The angular dependence raises a more difficult problem since it is determined by two contributions. The R^{-3} term results from both dipole–dipole and charge–quadrupole interactions. For both of them, at least in the particular case of the motions described in Fig. 3 (i.e., both dipoles in the same plane with $\theta_1 = \pm\theta_2$), the angular dependence is given by $(3\cos^2\theta - 1)$. Thus, dropping the last term in R^{-4}, the potential energy of the $(3e)^2\,(4e)^1$ configuration can be fitted to the expression (V_2 and R in a.u.)

$$V_2(R,\theta) = 0.0973R^{-2}\cos\theta - (1.9314/2R^3)(3\cos^2\theta - 1). \tag{4.4}$$

For $R = 8$ Å, this potential goes through a minimum at $\theta = 0°$ and $\theta = \pi$, and reaches a maximum at $\theta = 75.3°$. Comparison with the *ab initio* calculations is very satisfactory (Fig. 4).

In summary, the coherence between the *ab initio* calculations and the laws of the multipole expansion is satisfac-

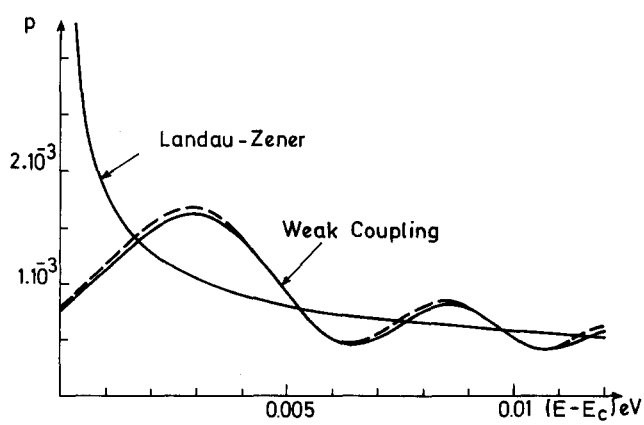

FIG. 6. Single-crossing transition probability as a function of the internal energy in the reaction coordinate for a value of $R_c = 7.18$ Å ($\lvert V_{12}\rvert = 3.3\times10^{-6}$ a.u.). The Landau–Zener approximation is compared with the weak-coupling formula. The full and broken curves correspond to the normal and deuterated compounds, respectively.

This article is copyrighted as indicated in the article. Reuse of AIP content is subject to the terms at: http://scitation.aip.org/termsconditions. Downloaded to IP: 139.165.205.242 On: Fri, 04 Sep 2015 14:32:57

tory. The analytical expressions (4.2) and (4.4) provide a convenient expression as a function of both radial and angular degrees of freedom.

V. NONADIABATIC COUPLING

Since the nonadiabatic interaction takes place at large internuclear distances, the diabatic basis set χ_i provides the best zeroth-order description. This implies a small value for the transition probability. The value of the latter is determined by the off-diagonal matrix element V_{12} between the two diabatic functions.

A CI program calculates the eigenfunctions of the electronic Hamiltonian H^{el}, i.e., the adiabatic wave functions ψ_i. However, adiabatic and diabatic wave functions coincide far away from the coupling zone.[24–26] Therefore, the CI expansions valid at $R = 26$ Å have been equated with the diabatic functions and have been used as follows:

$$\begin{aligned} V_{12}(R_c) &= \langle \chi_1 | H^{el}(R_c) | \chi_2 \rangle \\ &= \langle \psi_1(R = 26 \text{ Å}) | H^{el}(R_c) \\ &\quad \times | \psi_2(R = 26 \text{ Å}) \rangle. \end{aligned} \tag{5.1}$$

The results, calculated at several values of the internuclear distance R_c, are given in Table I. The coupling matrix element is seen to be quite small and to decrease very rapidly as a function of R_c. Thus, even a slight modification of R_c has important consequences on the magnitude of the transition probability and thus on the rate constant. As will be seen in Secs. VI and VII, this has important physicochemical consequences.

Since one has to deal with a weak coupling between two diabatic functions, at internal energies close to the threshold, the so-called weak coupling formula[26,27] is known to give much better results than the Landau–Zener equation. A graph giving the value of the single-crossing transition probability as a function of the internal energy in the reaction coordinate is given in Fig. 6 for a value of $R_c = 7.18$ Å ($|V_{12}| = 3.3\ 10^{-6}$ a.u.). The probability of leaving the initial diabatic electronic state [i.e., of switching from the $(3e)^3$ to the $(3e)^2\ (4e)^1$ configuration or vice versa] is seen to be quite small, of the order of 10^{-3}. Futhermore, the isotope effect is seen to be completely negligible. The explanation of the important effect detected experimentally has to be found elsewhere.

VI. EFFECTIVE POTENTIAL ENERGY CURVES

A fruitful approximation consists in applying an adiabatic separation, somewhat akin to the Born–Oppenheimer approximation, between the reaction coordinate R and the remaining degrees of freedom $\mathbf{u}$ to reduce the dimensionality of the problem.[28,29] If, as in the present case, the frequencies of the degrees of freedom $\mathbf{u}$ other than the reaction coordinate change slowly as they evolve from reactant to product, it is possible to treat them just as the electronic motion. The average potential, later on referred to as an effective channel potential, which is responsible for the motion of the slow coordinate R is then

$$V_w(R) = V(R) + E_w(R), \tag{6.1}$$

where $V(R)$ is the electronic potential and w is an energy label which is a combination of the internal quantum numbers associated with the degrees of freedom $\mathbf{u}$.

The simplest way of calculating the quantities $E_w(R)$ has been proposed by Quack and Troe[29] for an adiabatic reaction. Very briefly summarized, the channel energies result from an interpolation between the situation valid around the equilibrium position of the reactant and that valid for an infinite value of the reaction coordinate. This mimics the gradual conversion of some oscillators into rotations or translations. Two conservation laws are introduced: (i) conservation of the vibrational quantum numbers of the degrees of freedom which remain bound over the entire reaction path, and (ii) conservation of the total angular momentum.

Coming back to the case of the methylnitrite ion, we have to calculate these effective potential energy curves for each of the two electronic states involved in the problem. At large internuclear distances, the most important bending modes are those represented in Fig. 3. Both of them are doubly degenerate. At the values of R which will be considered, little error is incurred by considering them as a fourfold degenerate bending motion which transforms into rotation of the fragments as $R \to \infty$. The remaining degrees of freedom are intrafragment modes which remain practically unchanged when R varies from $\simeq 5$ Å to ∞.

The calculation of the effective potential energy curves will thus involve the transformation of the four quasidegenerate bending modes depicted in Fig. 3 plus the overall rotation into rotation and orbital motion of the fragments. For the $(3e)^3$ state, the bending modes result from the angular motion in an ion–dipole interaction [Eq. (4.2)], i.e., correspond to a hindered rotor. Since no analytical solution to the Mathieu equation exists,[30] we have parameterized it by a Pöschl–Teller expression

$$V(\theta) = -V_0/\cosh^2(\theta/a) \tag{6.2}$$

which admits a simple analytical solution.[31] The parameter a defines the curvature of the potential well. The interpolation formula which has been used to calculate the effective potential curves for the $(3e)^3$ diabatic state is

$$\begin{aligned} V_w^1(R) = &-1.0642R^{-2} + (n+2)h\nu(R) \\ &- (n+m+2)(\hbar^2/4I_{XY}a^2) \\ &+ [j_1(j_1+1) + j_2(j_2+1)](\hbar^2/2I_{XY}) \\ &\times [1 - C(R)] + P(P+1)[\hbar^2/2I(R)]. \end{aligned} \tag{6.3}$$

In this equation,

$$\nu(R) = (\hbar/8\pi I_{XY}a^2)\{[16I_{XY}V_0(R)a^2/\hbar^2] + 1\}^{1/2} \tag{6.4}$$

$V_0(R)$ is the potential barrier [Eq. (4.2) and (6.2)], $n = \Sigma\, n_i$, and $m = \Sigma\, n_i^2$, where n_i is the vibrational quantum number of a particular member of the fourfold degenerate oscillator. Several moments of inertia have to be defined. For large values of the distance R, the molecular ion has been approximated by a set of two identical rigid rotors XY (Fig. 7),

$$I_{XY} = m_X m_Y r_{XY}^2/(m_X + m_Y) \tag{6.5}$$

This article is copyrighted as indicated in the article. Reuse of AIP content is subject to the terms at: http://scitation.aip.org/termsconditions. Downloaded to IP: 139.165.205.242 On: Fri, 04 Sep 2015 14:32:57

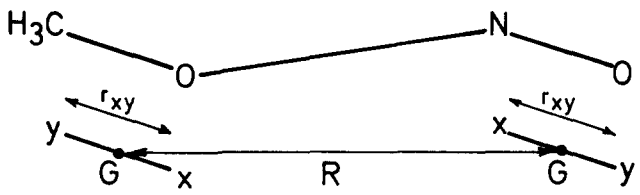

FIG. 7. The CH_3ONO^+ ion approximated, for large values of R, by a set of two rigid rotors XY.

with $m_X = 15$ daltons, $m_Y = 15.5$ or 17 daltons for the normal and deuterated compounds, respectively. The distance $r_{XY} = 1.22$ Å.

$$I(R) = 2m_X(R/2 - GX)^2 + 2m_Y(R/2 + GY)^2, \tag{6.6}$$

where GX and GY are defined in Fig. 7.

The quantum numbers j_1 and j_2 are introduced for the angular momenta of each fragment, J and l for the total and orbital angular momenta. Conservation of angular momentum is expressed by the vectorial equation

$$\mathbf{J} = \mathbf{j}_1 + \mathbf{j}_2 + \mathbf{l}. \tag{6.7}$$

P is a rotational pseudoquantum number[29] obtained by interpolation

$$P = JC(R) + l[1 - C(R)]. \tag{6.8}$$

The remaining problem concerns the specification of the switching function $C(R)$ which determines the way a vibrational degree of freedom is turned into rotation as R increases

$$\nu(R) = C(R)\nu(R_{eq}) \tag{6.9}$$

with the conditions $C(R_{eq}) = 1$ and $C(\infty) = 0$. In their work on neutral systems,[29] Quack and Troe have used an exponential switching function reminiscent of a Morse potential,

$$C(R) = \exp[-\alpha(R - R_{eq})], \tag{6.10}$$

where α is an empirical parameter. However, for systems involving long-range forces, the transition between vibration and rotation is much more gradual and other choices are preferable.[32] In the problem at hand, it is easy to deduce from the properties of the Pöschl–Teller potential[31] a function having the desired properties

$$C(R) = [V(R,0)/D]^{1/2}, \tag{6.11}$$

where D is the dissociation energy of the CH_3ONO^+ ion in the diabatic $(3e)^3$ state.

For the $(3e)^2\,(4e)^1$ configuration, the potential energy surface is very flat in the range of interest. Therefore, the energy levels will be modeled by a system of two free rotors. This amounts to setting $C(R)$ equal to zero in Eq. (6.3). One then gets

$$V_w^2(R) = -0.0973R^{-2} - 1.9314R^{-3} + [j_1(j_1+1) + j_2(j_2+1)][\hbar^2/2I_{XY}] + l(l+1)[\hbar^2/2I(R)]. \tag{6.12}$$

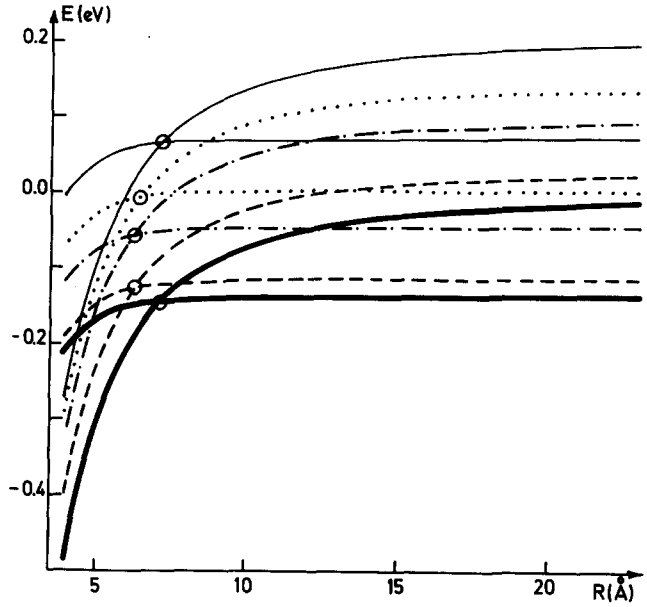

FIG. 8 Effective potential energy curves of the CH_3ONO^+ ion along coordinate R. Heavy line: $w = 1$; broken line: $w = 611$; dash–dots: $w = 4600$; dots: $w = 8000$; light line: $w = 10\,300$. The energies are measured from the asymptotic value of the $(3e)^3$ potential energy curve (with inclusion of its zero-point energy).

Numerical values of $\nu(R)$ [for electronic state $(3e)^3$] and of $B(R) = [\hbar^2/2I(R)]$ [for electronic state $(3e)^2\,(4e)^1$] are given in Table II.

The effective potential energy curves of the 10 300 lowest energy channels of CH_3ONO^+ in both electronic states have been calculated for a fixed value of $J = 0$. A few of them are represented in Fig. 8. For the lowest possible channel ($w = 1$), the crossing takes place at 7.18 Å. It is most important to note that, as w increases, R_c first shifts toward smaller values (down to 6.16 Å for $w \simeq 4000$), and increases again up to a value of 7.16 Å for $w = 10\,300$. The statistical treatment to be described in Sec. VII requires a knowledge of the coupling matrix element V_{12} (which is a sensitive function of R_c—see Table I) as a function of E_d, that part of the internal energy which goes into the four degenerate bending modes. [Since $E_d = nh\nu(R)$ is a function of R, it was decided to determine it at a value of $R = 6.7$ Å, i.e., right in the middle of the range of variation of R_c]. The results given in Fig. 9 for CH_3ONO^+ show that the nonadiabatic transition probability can be expected to depend very sensitively on E_d. This fact will be found to play a decisive role in the explanation of the constancy of the predissociation rate constant [point (e) of the introduction]. The same calculations were repeated for the CD_3ONO^+ isotopomer. The curve corresponding to Fig. 9 is very slightly displaced, but the practical consequences of this shift on the transition probability are insignificant.

VII. THE PREDISSOCIATION RATE CONSTANT

A. The statistical formulation

The off-diagonal matrix element V_{12} which determines the transition probability between the two diabatic surfaces

This article is copyrighted as indicated in the article. Reuse of AIP content is subject to the terms at: http://scitation.aip.org/termsconditions. Downloaded to IP: 139.165.205.242 On: Fri, 04 Sep 2015 14:32:57

has been seen (Table I) to be very small. However, even a weak interaction can give rise to a substantial value of the rate constant if the region of nonadiabatic interaction is crossed many times by the nuclear trajectories. During the time lag necessary for enough energy to flow into the reaction coordinate, the system executes a complicated Lissajous motion in the course of which the seam between the diabatic surfaces is crossed many times. This problem has been studied by Zahr, Preston, and Miller[33] and more recently by us[34] to obtain a simple statistical expression of the rate constant of a nonadiabatic unimolecular reaction.

Two related quantities, viz., the frequency ν^{cr} at which the seam is crossed, as well as the nonadiabatic (predissociation) rate constant $k^{pred}(E)$ can be expressed as phase space integrals over a microcanonical ensemble. This finally reduces to very simple expressions involving densities of states. In the simplest possible case, a distinction is introduced between the reaction coordinate R and a set of n_u degrees of freedom **u**, which we call "spectators". (The exact meaning of this term will be discussed later on). Consider a potential energy curve (resulting from a cross section along the reaction coordinate R) which admits a dissociation asymptote at energy E_0, and assume that it is further crossed by a second potential energy surface at energy E_c. At a given internal energy E, the frequency of crossing the seam ν^{cr} is given by[34]

$$\nu^{cr}(E) = \{2G_u^*(E-E_c) - G_u^*(E-E_0)\}/hN(E). \tag{7.1}$$

In this formula, which closely resembles the RRKM equation,[9] the integrated density of states $G_u^*(E)$ is equal to the total number of states of a fictitious system having n_u degrees of freedom between 0 and E.

$$G_u^*(E) = \int_0^E dE_u\, N_u^*(E_u). \tag{7.2}$$

The asterisk indicates that, just as in conventional transition state theory,[9] the densities of states are to be calculated with vibrational frequencies and moments of inertia evaluated at the crossing point R_c.

The predissociation rate constant then adopts a very simple expression[34]

$$k^{pred}(E) = \nu^{cr}(E)\langle p\rangle_E, \tag{7.3}$$

where $\langle p\rangle_E$ represents a microcanonical average of the probability p of undergoing a transition between the two weakly coupled diabatic states. In the present case, p can be calculated[26,27] either by the simple Landau–Zener equation (which is known to fail at low internal energies) or, preferably, by the weak coupling formula. One gets

$$\langle p\rangle_E = \left\{2\int_0^{E-E_c} dE_u\, N_u^*(E_u)p(E-E_c-E_u) - \int_0^{E-E_0} dE_u\, N_u^*(E_u)p(E-E_c-E_u)\right\} \Big/ \{2G_u^*(E-E_c) - G_u^*(E-E_0)\}. \tag{7.4}$$

Another equivalent form is possible:

$$k^{pred}(E) = [1/hN(E)]\left\{2\int_0^{E-E_c} dE_u\, N_u^*(E_u)p(E-E_c-E_u) - \int_0^{E-E_0} dE_u\, N_u^*(E_u)p(E-E_c-E_u)\right\}. \tag{7.5}$$

Equations (7.4) and (7.5) are very similar to the fundamental equation of RRKM theory,[9] valid for adiabatic reactions, and reduce to it in limiting cases.

$$k^{RRKM}(E) = [1/hN(E)]\int_0^{E-E_0} dE_u\, N_u^{\ddagger}(E_u) = G_u^{\ddagger}(E-E_0)/hN(E). \tag{7.6}$$

In both adiabatic and nonadiabatic reactions, the rate constant is expressed as a ratio, whose denominator is equal to $hN(E)$, where $N(E)$ is the density of states (in units energy^{-1}) of the reactant. The numerator implies in both cases a summation over all the possible exit channels. The crossing seam between the two diabatic states is found to play a role similar to that of the usual transition state. However, in the RRKM theory, it is sufficient to count the number of open channels. In the extension to nonadiabatic reactions, the contribution of each channel is weighted by a transition probability which plays the same role as the transmission coefficient introduced by Eyring and nearly always disregarded since.[9]

B. Displaced degrees of freedom

However, there exist severe conditions for Eqs. (7.1), (7.3), and (7.5) to be valid. Firstly, the interaction has to be sufficiently weak for the global probability of staying in the initial diabatic state to be equal to a product of individual probabilities. Secondly, the statistical treatment is enormously simplified if the seam can be represented by the simple equation $R = R_c$. This is true only if the diabatic potential energy surfaces are locally identical around the crossing seam along all coordinates **u** other than the reaction coordinate R. In particular, the equilibrium position of all the degrees of freedom **u** must be identical in both electronic states.

The first condition is fulfilled in our case, but the second is not. As shown in Fig. 1, the equilibrium positions of one of the bending motions are very different in each electronic state.

A stratagem will now be proposed, which bypasses the second requirement. It consists in going back to another treatment of the electronic predissociation of polyatomic molecules developed by Caplan and Child[35] (also valid for weak interactions only). The predissociation width $\Gamma(1n)$ (or the rate constant) of a particular vibronic initial state $(1n)$ (the symbol 1 refers to the electronic state, whereas n, represents a collection of vibrational quantum numbers) is given by a summation over all the possible final states of the other electronic state (labeled 2)

$$\Gamma(1n) = \sum_m \Gamma(1n,2m). \tag{7.7}$$

When the coupling is weak, each contribution $\Gamma(1n,2m)$ is given by an extension of Fermi's golden rule.[35] When the electronic matrix element V_{12} is constant, or can at

This article is copyrighted as indicated in the article. Reuse of AIP content is subject to the terms at: http://scitation.aip.org/termsconditions. Downloaded to IP: 139.165.205.242 On: Fri, 04 Sep 2015 14:32:57

least be replaced by an average value in the region of nonadiabatic interaction, the Condon approximation can be invoked. Moreover, according to an approximation widely used in chemical kinetics, the remaining multidimensional Franck–Condon integral can be split (totally or partly) into a product of one-dimensional overlap integrals between vibrational wave functions. It is then possible, if the behavior of a certain degree of freedom is particularly troublesome, to split off its contribution and to express the rate constant as a product between two factors. The first one is a Franck–Condon factor. The second factor is the rate constant of a fictitious molecule having one degree of freedom less than the original molecule, and for which the statistical treatment described in Sec. VII A can be applied. To be more specific, let us consider a particular degree of freedom characterized by different equilibrium positions in the two electronic states, and let us call y its internal coordinate. Thus, the set $\mathbf{q}$ of the internal degrees of freedom is partitioned as follows: $\mathbf{q} = \{R,y,\mathbf{u}\}$. If, as in the present case, the coupling matrix element V_{12} can be considered to be independent of y, then

$$\Gamma(1n,2m) = |\langle v_y|v_y'\rangle|^2 \Gamma(1n',2m'). \tag{7.8}$$

The total width (or rate constant) then follows from the previous equations

$$k_{1n}^{\text{pred}} = \Gamma(1n)/\hbar = (1/\hbar)\sum_m \Gamma(1n,2m). \tag{7.9}$$

The microcanonical rate constant $k(E)$ we are looking for is given by an average over all the initial states $1n$ having the same energy. The symbols n and m represent a collection of vibrational quantum numbers (with v_y being part of n and v_y' being part of m). If it turns out that all the possible combinations which occur in practice give rise in the microcanonical average to the same Franck–Condon factor $|\langle v_y|v_y'\rangle|^2$, then it is possible to factorize it out and to write

$$k^{\text{pred}}(E) = |\langle v_y|v_y'\rangle|^2 \tilde{k}(E), \tag{7.10}$$

with $\tilde{k}(E)$ being a statistical predissociation rate constant relative to a fictitious molecule having $(3N-7)$ degrees of freedom (including the reaction coordinate R but excluding the displaced degree of freedom y).

Such a factorization is possible in the particular case studied here. In the CH_3ONO^+ problem, the degree of freedom y is the motion which transfers a hydrogen atom from carbon to oxygen (Fig. 1). Its probable frequency is above 1000 cm^{-1}, i.e., very high with respect to the low energy ($\simeq 40\ cm^{-1}$) fourfold degenerate bending mode (Table II). The latter degrees of freedom thus absorb nearly all of the internal energy. Therefore, at least not too far above the threshold, the excitation of these fourfold degenerate bending modes will be overwhelmingly favored on a statistical basis, whereas that of the displaced degree of freedom can be neglected. Thus, for all practical purposes, $v_Y = 0$, and Eq. (7.10) can be written

$$k^{\text{pred}}(E) = |\langle 0|v_y'\rangle|^2 \tilde{k}(E). \tag{7.11}$$

A crude estimate of the Franck–Condon factor can be obtained as explained by Bandrauk and Laplante.[36] The slopes of the potential energy curves have been estimated from *ab initio* calculations.[13–18] The vibrationless level $v_y = 0$ is below the crossing point. The following values are obtained for the Franck–Condon factor: 1.4×10^{-2} for the normal compound and 1.6×10^{-3} for the deuterated species. The isotope effect is equal to 8.8. This number is very approximate, but its physical meaning is clear. This fairly large ratio results from the fact that the overlap describes a tunneling process which leads to a much smaller value for the deuterated compound.

C. Energy dependence of the crossing point

It has been seen in Sec. VI that the excitation of the fourfold degenerate bending motion induced a change in the position of the crossing point R_c (Fig. 9). Since the coupling matrix element V_{12} depends critically on R_c (Table I), this has important consequences on the transition probability. Therefore, in order to take care of this additional complication, the internal degrees of freedom $\mathbf{q}$ have to be partitioned as follows: $\mathbf{q} = \{R,y,\mathbf{d},\mathbf{v}\}$. In this notation, R is the reaction coordinate, y is the degree of freedom which has a different equilibrium position in the two electronic states (the HCO bending mode), $\mathbf{d}$ represents the internal degrees of freedom whose excitation modifies V_{12}, and $\mathbf{v}$ the remaining spectator degrees of freedom which just increase the phase space. The fictitious rate constant $\tilde{k}(E)$ pertains to the pseudomolecule $\{R,\mathbf{d},\mathbf{v}\}$. The derivation of the rate constant has been given elsewhere.[34] One obtains as a final result

$$k^{\text{pred}}(E) = [1/h\tilde{N}(E)]\,|\langle 0|v_y'\rangle|^2 \int_0^{E-E_c} dE_v\, N_v^*(E_v) \times \left\{2\int_0^{E-E_c-E_v} dE_d\, N_d^*(E_d)p[R_c(E_d)] - \int_0^{E-E_0-E_v} dE_d\, N_d^*(E_d)p[R_c(E_d)]\right\}. \tag{7.12}$$

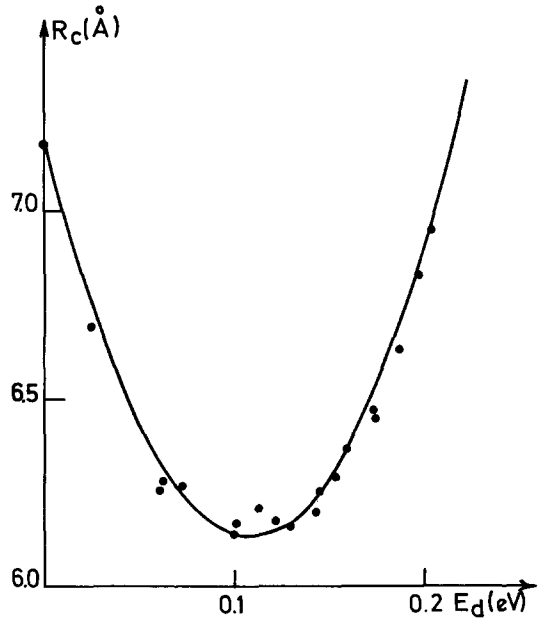

FIG. 9. Position of the crossing point R_c as a function of the energy E_d in the four quasidegenerate bending modes for CH_3ONO^+.

This article is copyrighted as indicated in the article. Reuse of AIP content is subject to the terms at: http://scitation.aip.org/termsconditions. Downloaded to IP: 139.165.205.242 On: Fri, 04 Sep 2015 14:32:57

TABLE II. Values of the fundamental frequency of the fourfold degenerate bending motion [in the electronic state $(3e)^3$] and of the rotation constant $B(R)$ [of the electronic state $(3e)^2(4e)^1$] for different values of the coordinate R.

R [Å]	$\nu(R)$ [cm^{-1}]	$B(R)$ [cm^{-1}]
5	62	0.077
6	52	0.048
8	39	0.024
10	31	0.014
12	26	0.010
15	20	0.006
20	15	0.003
25	12	0.002

In this expression, the tilde affixing the symbol $\tilde{N}(E)$ in the denominator is a reminder of the fact that the density of states has to be calculated for a $(3N-7)$ dimensional system, i.e., after withdrawal of degree of freedom y which is excluded from the statistical treatment. The symbol $p[R_c(E_d)]$ denotes the nonadiabatic transition probability. It can be calculated either from the Landau–Zener equation or, preferably, from the weak coupling formula.[26,27] The appropriate nuclear velocity is $[2(E-E_d-E_v-E_c)/\mu]^{1/2}$.

VIII. THE CH_3O+NO^+ CHANNEL

This reaction takes place on a single (diabatic) surface, that of electronic configuration $(3e)^3$. The predissociation rate constant can thus be studied by the conventional RRKM theory [Eq. (7.6)]. Since the potential energy curve of the $(3e)^3$ state raises continuously without going through a maximum (Fig. 5), there is no obvious position for the transition state. The crudest version of the variational transition state theory, i.e., the method of Bunker and Pattengill[37] which consists in minimizing the numerator of Eq. (7.6) has been adopted. This requires a knowledge of the variation of the frequency of the fourfold degenerate bending mode with the coordinate R; this has been given in Table II. The other frequencies remain constant as a function of R. They are intrafragment frequencies which have been taken from Refs. 14 and 38 (Table III). The adaptation to the deuterated compound has been inspired from a standard compilation.[39]

As expected from previous calculations,[40] the position of the transition state turns out to be energy dependent. The lower the internal energy E, the looser the transition state. In the present example, the transition state is found to be extremely loose close to threshold ($R^\ddagger = 38$ Å at $E = E_0 + 0.004$ eV). As E increases, the abscissa $R^\ddagger$ of the transition state along the reaction coordinate moves toward shorter values ($R^\ddagger = 15$ Å at $E = E_0 + 0.029$ eV, and $R^\ddagger = 11$ Å at $E = E_0 + 0.054$ eV). Very similar values of $R^\ddagger$ are found for CH_3ONO^+ and for CD_3ONO^+. The isotope effect on the position of the transition state is found to be insignificant [although the quantities $G^\ddagger(E-E_0)$ are obviously different].

IX. RESULTS

The basic expressions to be calculated are Eqs. (7.12) [for reaction (1.1)] and (7.6) [for reaction (1.2)]. The following numerical data have been adopted[1,4]: $E_c = 0.55$ eV, $E_0 = 0.69$ eV (with energies measured from the equilibrium position of the ground state of CH_3ONO^+). The energy level densities have been calculated by the Beyer–Swinehardt exact counting procedure.[41] Those which appear in the denominator of Eqs. (7.6) and (7.12) have to be calculated from the same set of vibrational frequencies, appropriate to the $(3e)^3$ state, except for the difference in the dimensionality of $N(E)$ and $\tilde{N}(E)$. The numerical values (inspired from spectroscopic results on the neutral molecules[42]) can be found in Table IV. The reaction coordinate has been treated as an anharmonic oscillator. The same thing applies to the CH stretching vibrational energy levels which converge to the CH_2ONO^+H asymptote. The frequencies of the CON and ONO bending modes have been halved to account for the double minimum effect.[43] Finally, the CH_3/CD_3 torsional levels have been replaced by a free rotor. The partial density of states $N_d^*(E_d)$ has been calculated from the energy levels of the anharmonic Pöschl–Teller potential at a fixed value of $R = 7.18$ Å. For the calculation of $N_v^*(E_v)$ we have used the intrafragment frequencies given in Table III.

The four rate constants $k^{\text{pred}}_{CX_3O^+}$ ($X = H$ or D) and $k^{\text{RRKM}}_{NO^+}$ from each isotopomer as well as the corresponding branching ratios are represented in Figs. 10 and 11 as a function of the internal energy E. However, in order to compare our calculated results with the experimental data,[1,8] it is necessary to convolute them first with a reasonable apparatus function. The latter results from the fact that, among other things, the energy of the analyzed photoelectrons is not strictly equal to zero. The apparatus function which we have used is similar to that proposed by Stockbauer,[44] with a width of 30 meV (FWHM) and a tail extending up to 300 meV.

X. DISCUSSION

Figures 12 and 13 show that this convolution brings the breakdown graphs calculated in the present work in reasona-

TABLE III. Intrafragment frequencies[14,38,39] of Ch_3O, CD_3O, and NO^+ (in cm^{-1}).

CH_3O:	2950,2930, 2870,1360, 1330, 1320, 1150, 1100, 1020.
CD_3O:	2200, 2200, 2070, 960, 960, 940, 940, 880, 840.
NO^+:	1609.

TABLE IV. Frequencies (in cm^{-1}) used for the calculation of $N(E)$ and $\tilde{N}(E)$. The underlined frequency is that of the isomerization mode (called y in the text).

CH_3ONO^+:	3010, 2990, 2890, 1509, 1360, 1330, <u>1320</u>, 786, 720, 510, 450, 210, 104, 49.
CD_3ONO^+:	2250, 2160, 2090, 1508, 960, 940, <u>920</u>, 750, 680, 430, 380, 203, 99, 47.

This article is copyrighted as indicated in the article. Reuse of AIP content is subject to the terms at: http://scitation.aip.org/termsconditions. Downloaded to IP: 139.165.205.242 On: Fri, 04 Sep 2015 14:32:57

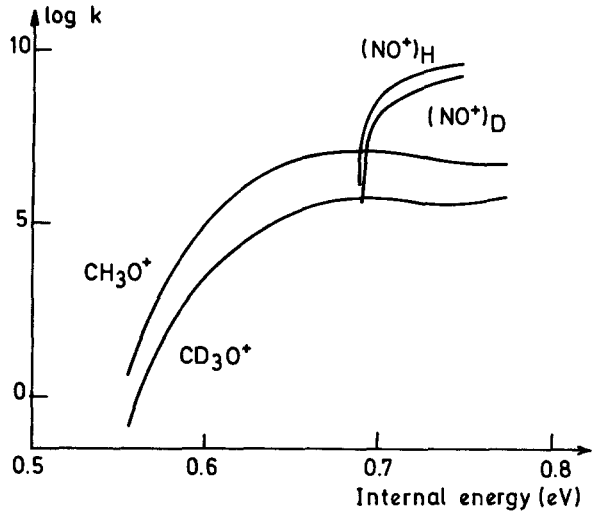

FIG. 10. Rate constants k^{pred} and k^{RRKM} relative to each isotopomer as a function of the internal energy.

ble agreement with those measured by Gilman *et al.*[1] Furthermore, after completion of this work, we have received information about the new experimental data obtained by Baer and Dutuit.[8] Their breakdown graph indicates that a third channel is open:

$$CX_3ONO^+ \rightarrow CX_2ONO^+ + H \quad (X = H \text{ or } D) \tag{10.1}$$

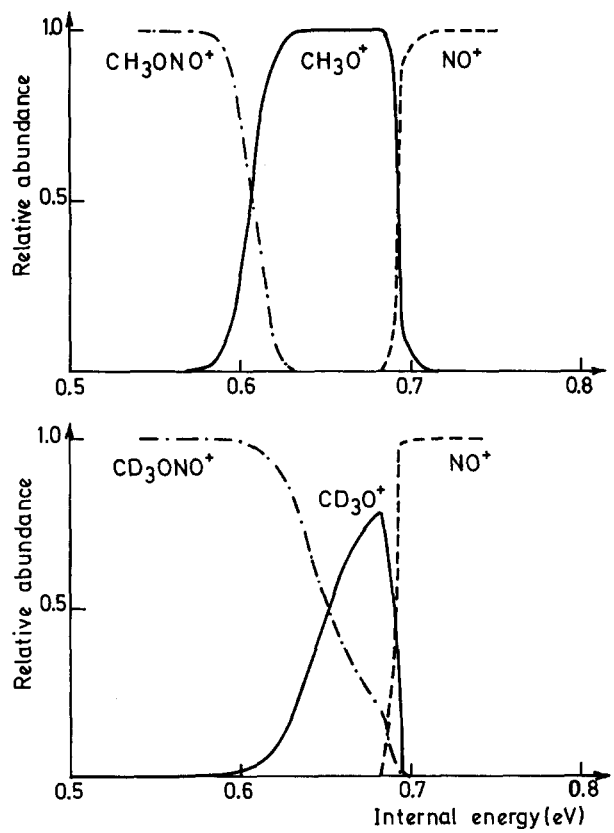

FIG. 11. Calculated breakdown curves corresponding to the dissociation of the normal and perdeuterated compounds.

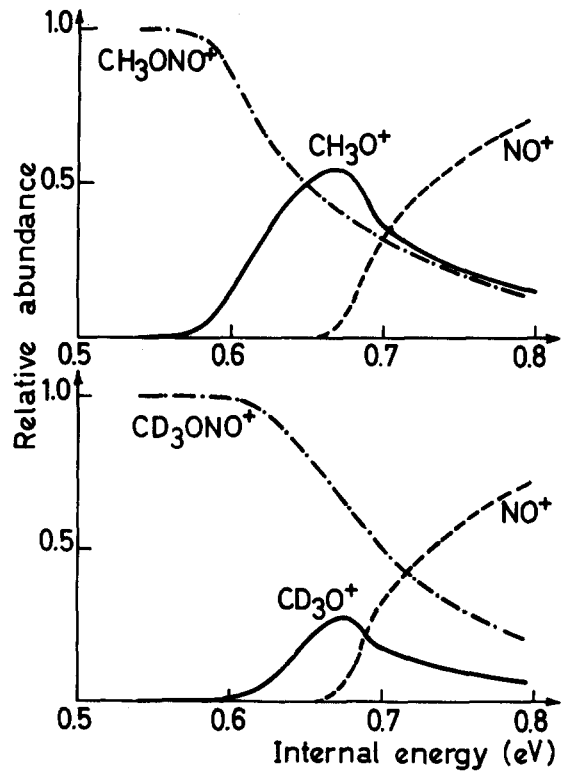

FIG. 12. Convoluted breakdown curves corresponding to the normal and perdeuterated compounds. The apparatus function has an asymmetric shape characterized by a width of 30 meV and a tail extending up to 300 meV.

The ion yield curve for the $[CH_3O]^+$ ion (whatever its structure) is very similar to that obtained by Gilman *et al.* Interestingly enough, that of $[CD_3O]^+$ is much more similar to our calculated results than to Gilman *et al.*'s measurements: the ion yield rises to a maximum value of 12%, whereas the maximum abundance obtained by Gilman *et al.* never exceeds 5%.

However, there are discrepancies between the experimental results obtained by the two groups. Baer and Dutuit have tried to get rid of the thermal energy distribution by a deconvolution operation. Although their original curves are very similar to Gilman *et al.*'s data and to our theoretical predictions, their deconvoluted breakdown graph is much less steep than our predictions: both fragments are present at the same internal energy over a fairly large energy range. The second point of disagreement concerns the rate constants which are found to increase rapidly with internal energy.

When it comes to proving or disproving a mechanism, it is always essential to distinguish carefully between the qualitative features of a model and the numerical calculations which follow. In our case, our numerical calculations of densities of states, of the matrix element V_{12} (Table I), of transition probabilities (Fig. 6), and of Franck–Condon factors [Eq. (5.1)], are admittedly crude. Thus, for instance, the exact value at which the rate constants level off (Fig. 10) cannot be predicted accurately. With this in mind, we proceed to a discussion which follows point by point the order adopted in the Introduction.

This article is copyrighted as indicated in the article. Reuse of AIP content is subject to the terms at: http://scitation.aip.org/termsconditions. Downloaded to IP: 139.165.205.242 On: Fri, 04 Sep 2015 14:32:57

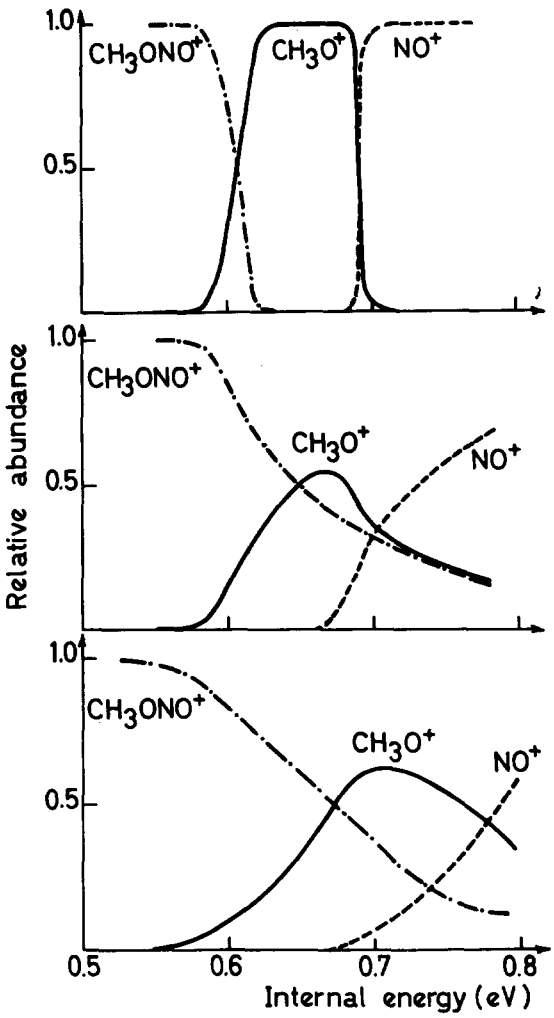

FIG. 13. Breakdown curves corresponding to the dissociation of the CH_3ONO^+ ion. Top: theoretical results; middle: the same after convolution; bottom: experimental results from Ref. 1.

(a) The weakness of the nonadiabatic interaction which is responsible for the production of the $[CH_3O]^+$ ions accounts for the specificity in favor of the NO^+ fragments. At internal energies higher than the threshold of reaction (1.2) the behavior of the system is in practice controlled by the shape of the $(3e)^3$ diabatic potential energy surface and the effects of the nonadiabatic coupling become entirely negligible.

(b) The ions $m/z = 31$ are born with a deformed H_3CO^+ structure (intermediate between the C_{3v} and the bridged structure, see Fig. 1), but immediately rearrange to the stable H_2COH^+ structure, a possibility envisaged by Burgers and Holmes.[3]

(c) The predicted isotope effect is considerable and remains large over an important energy range. We calculate a value of 27 for the ratio $(k_{CH_3O^+}/k_{CD_3O^+})$. Considering the basic equation (7.12), we see that part of it (i.e., a factor of 3) comes from the usual RRKM-like ratio $[N(E)]_D/[N(E)]_H$ between the densities of states.[9] The remaining factor of 9 comes from the Franck–Condon factor $|\langle 0|v_y'\rangle|^2$ associated with the HCO isomerization mode. The isotope effect on the value of the numerator of Eq. (7.12) is insignificant, at least at low energies. This results from the fact that most of the internal energy is absorbed by the fourfold degenerate bending mode whose frequency is not subject to a large isotope effect.

Thus, the existence of different equilibrium positions in the two electronic states between which the surface hopping occurs is at the origin of an important isotope effect, which is being maintained over a large energy range, and which is typical of nonadiabatic reactions. Conventional RRKM theory[9] can account for isotope effects which are large at threshold but which rapidly fade away as E increases. Ferguson's model[7] also involves tunneling along the isomerization coordinate y to account for effects (c) and (d), but through an adiabatic barrier.

In the next section, we shall discuss whether this considerable isotope effect can serve as a criterion to identify a nonadiabatic reaction.

(d) The low value of the rate constant of reaction (1.1) results from the smallness of the transmission coefficient, which is itself a consequence of the fact that the region of nonadiabatic interaction is located at very large internuclear distances.

(e) The rate constants $k_{CH_3O^+}$ and $k_{CD_3O^+}$ are expected to increase at first and then to reach rapidly a plateau whose value is substantially higher for the normal than for the deuterated compound. But, as already said, the exact value of these plateaux compared with the range where the rate constants can be studied experimentally cannot be determined accurately because of the uncertainties which affect our calculations. It might very well turn out that $k_{CD_3O^+}$ levels off at an energy which is slightly higher than our predicted value (Fig. 10). If so, both rate constants would be found to increase in the metastable range where the measurements can be carried out. The constancy of $k_{CH_3O^+}$ and of $k_{CD_3O^+}$ above a certain internal energy is accounted for by the shift of R_c towards larger values (Fig. 9). Even a small increase of R_c can induce a large decrease of V_{12} and hence of the transition probability. Thus, as the internal energy increases above a certain threshold, the number of reactive trajectories increases as well, but the probability of undergoing the surface hopping decreases. In other words, the phase space of the transition state increases with the internal energy, but each cell of this phase space is characterized by a nonadiabatic transition probability which decreases with E. Still equivalently, increasing the energy amounts to adding new but inefficient channels.

(f) We now come to the final observation which no doubt constitutes the most delicate point of the discussion. According to the laws of macroscopic kinetics, when two unimolecular reactions take place competitively from the same precursor, the reaction products are formed in a yield which is equal to the ratio of the rate constants (k_1/k_2), but they both appear with the same rate constant $(k_1 + k_2)$. This law is often considered as a test[1,4,10,45] for deciding whether both reactions are competitive or whether it is necessary to introduce an intermediate step (e.g., an isomerization) into the kinetic scheme.

We submit that the nonadiabatic model which has accounted for several remarkable features of the dissociation is not disproved by this argument. Using a quantum mechani-

This article is copyrighted as indicated in the article. Reuse of AIP content is subject to the terms at: http://scitation.aip.org/termsconditions. Downloaded to IP: 139.165.205.242 On: Fri, 04 Sep 2015 14:32:57

cal formalism, Mies and Krauss[46] have analyzed the validity of the laws of macroscopic kinetics with particular reference to the application of the transition state theory to mass spectrometric experimentation. They conclude that competitive decay will take place with equal rates only when all the resonances are characterized by the same total and partial widths. This is a severe restriction. If so, this would cast doubt about the significance of our calculated rate constants, displayed in Fig. 10. Work is currently in progress in this laboratory to investigate this point in more detail.

The calculation of breakdown diagrams is, however, free from this criticism, because the statistical formalism developed in Ref. 34 and summarized in Sec. VII amounts to calculating the microcanonical average of a branching ratio, as opposed to the ratio of two individual microcanonical averages which would lead to an incorrect result. We postpone the calculation of quantum laws expressing the (not necessarily exponential) rates of decay to a future publication. Nevertheless, we feel that the present calculations retain their value. The mechanisms which lower the value of the nonadiabatic transition probability as E increases (i.e., which make the high-energy channels less easily predissociated) can be expected to operate as well in a more elaborate quantum-mechanical calculation of the rates of decay.

XI. CONCLUSIONS

We now wish to depart somewhat from the particular case of the methylnitrite ion and its experimental uncertainties in order to discuss the problem in more general terms. Can some of the intriguing features which have been detected in the reactions serve as a criterion to distinguish nonadiabatic from adiabatic reactions?

First of all, we have to emphasize that the surprising effects can be accounted for by a statistical theory, and even by a transition state theory. There is no reason to express doubts about the establishment of a state of microcanonical equilibrium. The extension of the transition state theory which we have developed for nonadiabatic reactions is based on a classification of the internal degrees of freedom. It has been necessary to maintain a distinction among: the reaction coordinate R, the displaced degree of freedom y, the energy acceptor modes $\mathbf{d}$, and finally the remainder $\mathbf{v}$ which, until fuller information is available, it considered as a set of passive spectators. In addition, there is the everlasting problem of the external rotation which has been completely ignored here, since only the $J = 0$ states have been studied.

Coming back to the original question, there is no doubt that the nonadiabatic coupling can reduce the magnitude of a rate constant with respect to a more normal value. However, spectacular effects such as the strong isotope effect [point (c)], and the constancy of $k(E)$ [point (e)], require an interplay among three main factors: (i) the nonadiabatic nature of the reaction, (ii) the displacement of the equilibrium positions of the two potential energy surfaces along a degree of freedom y which involves the motion of a hydrogen atom, and (iii) the looseness of the critical configuration (i.e., the large value of R_c) which creates a sink of low-energy modes. The latter circumstance results itself (Fig. 2) from the smallness of the asymptotic energy gap ΔE_∞ between the dissociation asymptotes and from the fact that the two crossing diabatic states differ in their nature: short range for one, long range for the other. The classification of the degrees of freedom $\{R,y,\mathbf{d},\mathbf{v}\}$ results directly from the existence of these three factors.

The strong isotope effect is due to a combination of two circumstances which take place in parallel and reinforce each other, i.e., the normal (RRKM-like) effect on the density of states $N(E)$ and the tunnel effect due to the displacement of the equilibrium positions of the two potential energy surfaces. But the tunnel effect produces spectacular results only because of the existence of a sink of low-energy modes which maintains the motion along the displaced mode in the tunneling regime where the isotope effect is largest.

Similarly, a shift in the values of the position of the crossing point brings about a weak increase of the rate constant k as a function of E. This results from the different nature (short and long range) of the interaction potentials in each of the two crossing electronic states. Here again, the energy sink plays a leading role.

To summarize, one might say that the surprising effects result from the nonadiabatic interaction [factor (i)], that they are especially strong because of the difference in the equilibrium positions along the tumbling motion y [factor (ii)], and that they persist over a wide energy range because of the presence of a sink of low-frequency bending modes [factor (iii)].

ACKNOWLEDGMENTS

The authors are grateful to Professor T. Baer, Dr. P. Burgers, Dr. O. Dutuit, Professor E. Ferguson, Professor W. Forst, Professor G. Meisels, and Professor L. Radom for helpful discussions and correspondence. They wish to thank Dr. M. Th. Praet for her help with the *ab initio* calculations. B. L. N. is indebted to the F.N.R.S. (Belgium) for the award of a fellowship. This work has been supported by grants from the Belgian Government (Action de Recherche Concertée) and from the Fonds de la Recherche Fondamentale Collective.

[1](a) G. G. Meisels, T. Hsieh, and J. P. Gilman, J. Chem. Phys. **73**, 4126 (1980); (b) J. P. Gilman, T. Hsieh, and G. G. Meisels, *ibid.* **78**, 1174 (1983); (c) **78**, 3767 (1983).
[2]I. K. Ogden, N. Shaw, C. J. Danby, and I. Powis, Int. J. Mass Spectrom. Ion Proc. **54**, 41 (1983).
[3]P. C. Burgers and J. L. Holmes, Org. Mass Spectrom. **19**, 452 (1984).
[4]T. Baer and J. R. Hass, J. Phys. Chem. **90**, 451 (1986); T. Baer, Adv. Chem. Phys. **L14**, 111 (1986).
[5](a) H. Egsgaard, L. Carlsen, and S. Elbel, Ber. Bunsenges. Phys. Chem. **90**, 369 (1986); (b) M. L. McKee, J. Phys. Chem. **90**, 2335 (1986).
[6]J. C. Lorquet, C. Barbier, and B. Leyh-Nihant, Adv. Mass Spectrom. 10A, 71 (1986).
[7]E. E. Ferguson, Chem. Phys. Lett. **138**, 450 (1987).
[8]T. Baer and O. Dutuit, private communication; see Abstract for Synchrotron Meeting in Brookhaven (Nov. 1987).
[9]W. Forst, *Theory of Unimolecular Reactions* (Academic, New York, 1973).
[10]T. Baer, W. A. Brand, T. L. Bunn, and J. J. Butler, Faraday Discuss. Chem. Soc. **75**, 45 (1983); M. Panczel and T. Baer, Int. J. Mass Spectrom. Ion Proc. **58**, 43 (1984).
[11]G. G. Meisels (private communication).
[12]R. S. Berry, J. Chem. Phys. **27**, 1288 (1957); B. J. Botter, J. A. Kooter, and J. J. C. Mulder, Chem. Phys. Lett. **33**, 532 (1975); L. R. Kahn, P. J. Hay, and I. Shavitt, J. Chem. Phys. **61**, 3530 (1974).

This article is copyrighted as indicated in the article. Reuse of AIP content is subject to the terms at: http://scitation.aip.org/termsconditions. Downloaded to IP: 139.165.205.242 On: Fri, 04 Sep 2015 14:32:57

[13]G. F. Adams, R. J. Bartlett, and G. D. Purvis, Chem. Phys. Lett. **87**, 311 (1982).
[14]S. Saebo, L. Radom, and H. F. Schaefer III, J. Chem. Phys. **78**, 845 (1983).
[15]P. v. R. Schleyer, E. D. Jemmis, and J. A. Pople, Chem. Commun. **190**, (1978).
[16]J. D. Dill, C. L. Fischer, and F. W. McLafferty, J. Am. Chem. Soc. **101**, 6531 (1979).
[17]W. J. Bouma, R. H. Nobes, and L. Radom, Org. Mass Spectrom. **17**, 315 (1982).
[18]L. Radom (private communication).
[19]C. F. Jackels, J. Chem. Phys. **76**, 505 (1982).
[20]The program system MOLACH incorporates the MOLECULE Gaussian integral program and the ALCHEMY SCF and CI wave function generator programs. MOLECULE was written by Dr. J. Almlöf of the University of Uppsala, Sweden. ALCHEMY was written at the IBM San Jose Research Laboratory. The interfacing of these programs was performed by P. S. Bagus and U. I. Wahlgren. For a description of MOLECULE, see J. Almlöf, Proceedings of the Second Seminar of Computational Problems in Quantum Chemistry (Max-Planck-Institut, München, 1973), p. 14. For a description of ALCHEMY see P. S. Bagus, in *Selected Topics in Molecular Physics* (Chemie, Weinheim, 1972), p. 187.
[21]S. Huzinaga, J. Chem Phys. **42**, 1293 (1965); T. H. Dunning, *ibid.* **53**, 2825 (1970).
[22]J. M. Robbe and H. Lefebvre-Brion, J. Mol. Spectrosc. **90**, 439 (1981).
[23]F. P. Billingsley II, J. Chem. Phys. **62**, 864 (1975).
[24]M. Desouter-Lecomte, D. Dehareng, B. Leyh-Nihant, M. Th. Praet, A. J. Lorquet, and J. C. Lorquet, J. Phys. Chem. **89**, 214 (1985).
[25]M. Desouter-Lecomte, B. Leyh-Nihant, M. Th. Praet, and J. C. Lorquet, J. Chem. Phys. **86**, 7025 (1987).
[26]M. Desouter-Lecomte and J. C. Lorquet, J. Chem. Phys. **71**, 4391 (1979).
[27]J. B. Delos, J. Chem. Phys. **59**, 2365 (1973).
[28]J. O. Hirschfelder and E. Wigner, J. Chem. Phys. **7**, 616 (1939); M. A. Eliason and J. O. Hirschfelder, J. Chem. Phys. **30**, 1426 (1959).
[29]M. Quack and J. Troe, Berg. Bunsenges. Phys. Chem. **78**, 240 (1974); J. Troe, J. Chem. Phys. **75**, 226 (1981).
[30]H. Eyring, J. Walter, and G. E. Kimball, *Quantum Chemistry* (Wiley, New York, 1967), p. 358.
[31]S. Flügge, *Practical Quantum Mechanics* I (Springer, Berlin, 1971); D. Ter Haar, *Problems in Quantum Mechanics*, 3rd Edition (Pion, London, 1975); P. Senn, Chem. Educ. **63**, 75 (1986).
[32]J. Troe, J. Phys. Chem. **90**, 3485 (1986); J. Troe, Chem. Phys. Lett. **122**, 425 (1985).
[33]G. E. Zahr, R. K. Preston, and W. H. Miller, J. Chem. Phys. **62**, 1127 (1975).
[34]J. C. Lorquet and B. Leyh-Nihant, J. Phys. Chem. (in press).
[35]C. E. Caplan and M. S. Child, Mol. Phys. **23**, 249 (1972).
[36]A. D. Bandrauk and J. P. Laplante, J. Chem. Phys. **65**, 2592 (1976).
[37]D. L. Bunker and M. Pattengill, J. Chem. Phys. **48**, 772 (1968); W. L. Hase, Acc. Chem. Res. **16**, 258 (1983).
[38]B. Rosen, *Spectroscopic Data relative to Diatomic Molecules*, International Tables of Selected Constants (Pergamon, Oxford, 1970).
[39]T. Shimanouchi, Tables of Molecular Vibrational Frequencies, Natl. Stand. Ref. Data Ser., Natl. Bur. Stand. **39** (1972).
[40]H. Gaedtke and J. Troe, Ber. Bunsenges. Phys. Chem. **77**, 24 (1973).
[41]T. Beyer and D. F. Swinehart, Comm. Assoc. Comput. Mach. **16**, 379 (1973); S. E. Stein and B. S. Rabinovitch, J. Chem. Phys. **58**, 2438 (1973).
[42]F. L. Rook and M. E. Jacox, J. Mol. Spectrosc. **93**, 101 (1982); P. N. Ghosh and Hs. H. Günthard, Spectrochim. Acta Part A, **37**, 347 (1981); L. Farnell and J. F. Ogilvie, Proc. R. Soc. London Ser. A **381**, 443 (1982).
[43]G. Herzberg, *Molecular Spectra and Molecular Structure. Infrared and Raman Spectra of Polyatomic Molecules* (Van Nostrand, Princeton, 1968), Vol. II, p. 221.
[44]R. Stockbauer, J. Chem. Phys. **70**, 2108 (1979).
[45]H. Kühlewind, A. Kiermeier, and H. J. Neusser, J. Chem. Phys. **85**, 4427 (1986).
[46]F. H. Mies and M. Kraus, J. Chem. Phys. **45**, 4455 (1966).

This article is copyrighted as indicated in the article. Reuse of AIP content is subject to the terms at: http://scitation.aip.org/termsconditions. Downloaded to IP: 139.165.205.242 On: Fri, 04 Sep 2015 14:32:57